https://doi.org/10.31896/k.29.5
Original scientific paper
Accepted: 5 November 2025

Christian Clemenz
Boris Odehnal

Limits of Triangle Centers

Limits of Triangle Centers

ABSTRACT

The construction of a triangle center always produces central triangles which again allow for the construction of the respective center. Doing this infinitely many times may in some cases lead to a known triangle center, but in the vast majority, a new center will show up. The symbolic computational approach is limited in many cases due to the complexity of the computations. In order to overcome these difficulties, we shall start with numerical approaches towards several centers' limits. This gives rise to some conjectures which later allow for an exact determination of the limit of a triangle center.

Key words: triangle center, iterated construction, numerical simulation, limit

MSC2020: 51N20, 51Nxx, 68U05

Granične vrijednosti središta trokuta

SAŽETAK

Konstrukcija središta trokuta uvijek stvara središnje trokute koji ponovno omogućavaju konstrukciju odgovarajućeg središta. Ponavljanje ovog postupka beskonačno mnogo puta može u pojedinim slučajevima dovesti do poznatog središta trokuta, ali u velikoj većini slučajeva pojavit će se novo središte. Simbolički računski pristup je ograničen u mnogim slučajevima zbog složenosti izračuna. Kako bismo prevladali te teškoće, započet ćemo s numeričkim pristupima prema graničnim vrijednostima nekoliko središta. To dovodi do nekih pretpostavki koje kasnije omogućavaju točno određivanje granične vrijednosti središta trokuta.

Ključne riječi: središte trokuta, iterativne konstrukcije, numeričke simulacije, granična vrijednost

1 Introduction

1.1 Related and prior work

In classical and elementary geometry, usually constructions terminate after a finite number of steps. However, some constructions may invite us to repeat them not only once and we may ask ourselves what will happen if we repeat them infinitely many times. Since the constructions that we want to repeat infinitely many times follow the same recipe in each step, the thus produced geometric objects are determined by means of some algorithm. Under certain circumstances, we can expect that such infinitely many times repeated constructions will in the end lead to a useful result, *i.e.*, they produce a limit. Moreover, since the recipe does not change, we may discover a certain simple generation and construction of the limit. These could be, for example, a chain of similar figures (cf. [13]), a geometric sequence, perspectivities, and more as we shall see later. Many constructions in and around the triangle can be performed by means of linear or rational operations, many involve square roots (circle intersections from the constructive point of view), and some cannot be accessed by means of the classical tools (*e.g.*, Morley triangles and their centers).

The only algebraic approach towards iterated triangle center constructions can be found in [1]. There, the degree $d(f)$ of a triangle center $Z = f : \zeta(f) : \zeta^2(f)$ is defined with the help of Z's generating trilinear center function f. This degree either remains unchanged or changes to $d(-2)^{-k}$ for the respective center in the k-th step of the iteration. Unfortunately, the thus defined degree has no deeper geometric meaning and depends on the trilinear center function, *i.e.*, it yields different degrees for different but equivalent representations of the same center. As we shall see, the asymptotic behaviour of linear operators is sometimes crucial in understanding the limiting process of a triangle construction. In [3], this is done for simplices and discloses relations to matrix theory. [6] does not provide limits of triangle centers, but deals with the limit shape of central triangles in some cases. An intricate but nevertheless interesting approach using bivariate Fourier series for the representation of the limit of a point and iterated pedal triangles is given in [4].

1.2 Aims and contributions of the present note

The repeated center construction in a given triangle can be performed numerically in an easy way. We shall describe the implementation of our numerical simulations in Sec. 2. They allow for a flexible access to the limits of various centers under different assumptions of reference triangles. Among others, we can use the *standard reference triangle* with side lengths $a = 6$, $b = 9$, and $c = 13$ which allows us to compare resulting limits with C. KIMBERLING's *search table* in the Encyclopedia of Triangle Centers (cf. [7]). We will not give an exhaustive treatment of center limits. Just a few well-known and low indexed centers shall be studied. The numerical computations provide us with ideas how to construct the centers that emerge in the limit. In Sec. 3, we shall give exact proofs of what can be conjectured from the numerical experiments.

2 Numerical approach

2.1 Implementation details

In order to visually explore the behaviour of different center constructions, we developed an interactive program using the open source game engine Godot[1] which offers a flexible framework for scripting and displaying 2D graphics that is compatible with many different programming languages. We chose C# because of its easy access to external libraries and overall speed of development. Our program allows for the repeated numerical determination of the first eleven triangle centers listed in C. KIMBERLING's encyclopedia [7]. However, it can be extended to all those centers that have a geometric generation.

The repreated construction of a triangle center needs a new reference triangle in each step. In many cases, it is necessary to use the Cevian or the pedal triangle. Depending on the definition and construction of the center under consideration, a base triangle different from the latter two is chosen. We shall discuss this in more detail in Sec. 3. In our interactive program one can either choose the pedal triangle $\Delta_p(X_i)$ or the Cevian triangle $\Delta_C(X_i)$ related to the triangle center X_i as the starting triangle for the next step in the iteration. The reference triangle shall not be changed during the iteration. The Spieker point X_{10} is the only exception that uses its own construction method, which will be explained in Sec. 2.4.7.

[1]Godot Game Engine – https://godotengine.org

2.2 Precision

As with any numerical approach, calculations need to be of a certain precision to guarantee the robustness of and the confidence in the results. What kind of target precision is needed depends on multiple factors.

The first precision requirement stems from the values in C. KIMBERLING's search table. In their 6–9–13 triangle search table, a precision of twenty decimals is used. Typically, double precision floating point numbers are stored using 64 bits and can cover a very large range of numbers, in C# for example this range is $\sim 10^{-324}$ to 10^{308}. However, their maximum precision is only around 15–17 digits [11] and are, therefore, insufficient for our purpose. Additionally, C# provides the *decimal* numeric type that is recommended for higher precision, especially for values $-1 < x < 1$. This type can store up to 28–29 digits to the right of the decimal point. In theory, these values should be precise enough to store results that can be compared with search table values.

However, the second requirement is defined by the precision needed by the used mathematical operations. As values are expected to shrink rapidly, an even higher precision is needed to guarantee that operations still result in values that are robust according to the first requirement. After only very few iterations of repeated triangle construction, some *decimal* type results may already be indistinguishable from zero. Particularly, any construction that involves vector normalization or normal projection suffers greatly from low precision. In such cases, very small vector norms can lead to divisions by zero induced by rounding errors and prohibit any further iteration.

One way of tackling this problem is the use of decimal numbers with arbitrary precision. These are not included in most programming languages by default and may need to be imported from an external library. The *Extended Numerics* package for C# by ADAM WHITE [15] is such a library that includes an arbitrary *BigDecimal* type. It stores exponent and mantissa separately as integers and calculates in base 10 rather than using the usual binary format for floating point numbers. One particular feature of *BigDecimal* allows us to truncate the result of any operation to an arbitrary decimal point while still using the full potential range of decimals for the calculation itself. This offers the deliberate choice to reduce the precision in order to improve computation speed by introducing a certain degree of rounding errors without the risk of running out of precision during an operation. Unfortunately, this feature does not entirely prevent the numerical problems but rather delay them if further iterations are needed. As a default, we limit the precision to around 25–50 digits to keep the program we developed interactive. For our numerical results in Section 2.4.9, we opted for a higher precision.

2.3 First numerical results

Along with the visuals, we looked at a variety of different properties that could give further insight into the behaviour of the repeated construction. For the resulting triangles, we calculated the ratio of the side lengths and interior angles that can reveal whether there are any systematic changes in their overall shape, such as regularization or other obvious patterns. For the resulting centers, we create a curve that connects subsequent centers and calculate the distance of and angle between subsequent segments, respectively. These two properties give hints at the tendency to converge and if the centers are collinear. Putting all these values together may give insights on how to tackle these constructions algebraically. Additionally, we will also describe any intermediary centers that are contained in the search table if they are found during the construction, as these could also be valuable information.

Note that we primarily focused on the behaviour of the 6-9-13 triangle. Any findings we described below refer to this triangle unless stated otherwise. When looking up search values in KIMBERLING's search table, we assume a tolerance of 10^{-7}, meaning these values are likely to describe the same center if their absolute difference is smaller than this tolerance. We do so because numerical errors on either side may hide the fact that it may be the same center. This threshold was chosen empirically, as we found that differences are either noticeably larger than that or almost zero. A much smaller tolerance may be applicable, especially if we increase precision and iteration count.

A list of our calculated search values can be found in Table 1 at the end of this section.

2.3.1 Incenter X_1

Repeatedly constructing the incenter quickly leads to a regularization of the resulting triangles for both pedal and Cevian triangle construction (cf. Thm. 1). While both constructions seem to converge, neither of the two points determined numerically is contained in the search table. Only the incenter of the intouch triangle, *i.e.*, the incenter of the intouch triangle known as X_{177} (cf. [7, 8]) appears in the search table.

2.3.2 Centroid X_2

In the case of the centroid X_2, the medial triangle Δ_m of Δ equals the Cevian triangle $\Delta_C(X_2)$. Consequently, the second centroid is that of Δ_m which equals X_2. Hence, repeating the centroid construction with the Cevian triangle returns the centroid X_2 of Δ in the limit.

The pedal triangle construction on the other hand exhibits a different behaviour. It quickly regularizes the triangles after around four iterations, while the distance between each new centroid is indistinguishable from zero as early as seven iterations, finalizing the convergence. The point the centroids converge towards is not contained in the search table. On the second iteration the created center is X_{373}.

2.4 Circumcenter X_3

Repeating the circumcenter construction using the Cevian triangles as the reference triangles, we observe an overall chaotic behaviour. The triangle center X_{23719} is the circumcenter of Δ_m and appears as the circumcenter in the second step of the iteration (cf. Fig. 1).

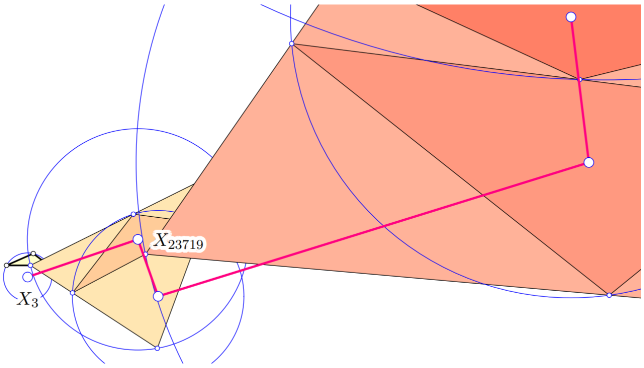

Figure 1: *The chaotic path of the circumcenter of its predecessor's Cevian triangle: Only two points in the sequence are known.*

In contrast, the pedal triangle construction exhibits a very obvious convergence towards the centroid X_2. Now, all intermediate points are collinear centers located on the Euler line. The first five centers after following the circumcenter can be found in the search table and are in order of their construction $X_5, X_{140}, X_{3628}, X_{16239}, X_{61877}$. They lie on the Euler line as well as all subsequent centers do, see Thm. 2.

2.4.1 Orthocenter X_4

In this particular case, we have $\Delta_C(X_4) = \Delta_p(X_4) = \Delta_o$. Let now $\Delta_o = A'B'C'$ such that $A' \in [B,C]$ (cyclic). Further, $\sphericalangle AA'C = \sphericalangle BB'C = \frac{\pi}{2}$. If α, β, γ denote the interior angles of Δ, then $\sphericalangle A'AC = \sphericalangle B'BC = \frac{\pi}{2} - \gamma$, since A, C', A', C and B, C', B', C are concyclic. Thus, $\sphericalangle A'C'B' = \sphericalangle A'AC + \sphericalangle B'BC = \pi - \gamma$ (cyclic). From that, we can deduce that the interior angles of the k-th orthic triangle are equal to

$$\alpha(k) = (-1)^{k+1}\pi + (-2)^k\alpha \quad \mod 2\pi \quad \text{(cyclic)}.$$

This means that the orthic triangles rotate with exponential speed. Besides, it is by no means guaranteed that the orthic triangle at some level stays within the interior of its predecessor. The same holds true for the orthocenter.

A very special result is due to NEUBERG (see [2]): The third pedal triangle of a fixed point with respect to a given triangle Δ is similar to Δ. Unfortunately, NEUBERG's result

deals with a fixed point whose pedal triangles are studied. Here, and in the following, the point whose pedals or Cevians are used changes from step to step.
Clearly, the orthocenter reaches a limit in the case of an equilateral triangle Δ. We shall not discuss right and isosceles triangles here.
The second step of the iteration, yields X_{52} as the orthocenter of the orthic triangle which fits with the results in [7, 8].

2.4.2 Nine-point center X_5

Constructing this center repeatedly exhibits very chaotic behaviour for both construction types of reference triangles. While the construction based on $\Delta_C(X_5)$ does not seem to have any obvious patterns, the construction based on the pedal triangle appears to regularize the reference triangles. This happens much slower compared to other center constructions that do so. The second nine-point center found using pedal triangles equals X_{13365} which is referred to as *Point Beid 48* in [7].

2.4.3 Symmedian point X_6

The Symmedian point has a very interesting behaviour. While the Cevian triangle construction only leads to a regularization, the pedal triangle construction has a more unique behaviour. Its center points move on a zig-zag curve with a constant interior angle of 129.4365 degrees finally converging towards the center X_{1285}. Notably, on the second step of the iteration the created center can be recognized as X_{18907} in the search table.

2.4.4 Gergonne point X_7

The Gergonne point exhibits a regularization when using the Cevian triangles and seems to converge towards a point not contained in the search table.
The pedal triangle construction however looks a lot more interesting as it seems to have some underlying pattern which can be seen in Figure 2. The constructed centers seem to be almost collinear visually, but on further inspection the angle between iterations is around 178.1–178.3 degrees. The resulting triangles visually seem to alternate between two different shapes, one of them being similar to the starting triangle. However, numerically there is always an additional small deviation from those shapes after each iteration.

2.4.5 Nagel point X_8

When using Cevian triangles, the construction of the Nagel point stops after only three iterations because the resulting triangles rapidly collapse to a line and calculations become unstable. Even on a precision higher than the limit of the interactive program, further iterations do not make sense.
The same is true for the pedal triangles, however, the construction is possible for a few more iterations. If not for the numerical instability, this type of construction would seem to converge as the centers seem to follow a zig-zag curve with each additional line of the curve slowly getting shorter and angles between them getting smaller which can be seen in Figure 3.

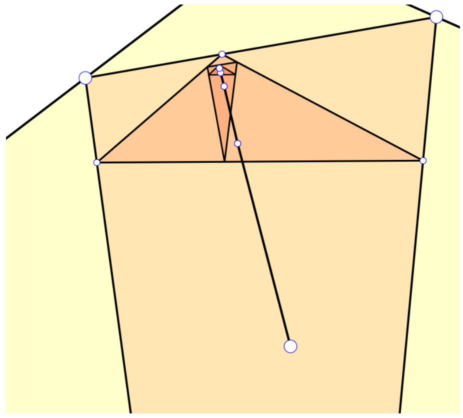

Figure 2: *The trail of the Gergonne point X_7: Only four steps of the iteration are to show that the second and fourth pedal triangle are almost similar to Δ.*

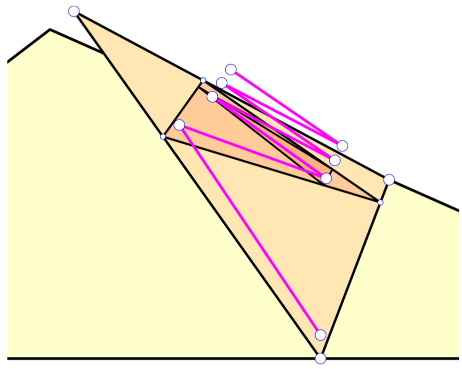

Figure 3: *The oscillating path of the Nagel point X_8: The corridor of "even" and "odd" points is slowly getting narrower.*

2.4.6 Mittenpunkt X_9

Similar to the Nagel point, the construction of the Mittenpunkt using Cevian triangles stops after only three steps. Both share a similar construction using excircles and the problem of triangles collapsing. Using pedal triangles instead leads to a quick triangle regularization and the centers seem to converge towards a point not found in the search table.

2.4.7 Spieker center X_{10}

As briefly mentioned above, we treat the repeated construction of the Spieker center differently. This is because the construction of this center naturally already leads to a triangle that is suitable for repeated use. As the Spieker point being the incenter of a triangle's medial triangle, it is convenient to use the intouch triangle of the medial triangle for repeated construction of the Spieker center. This subsequently regularizes the used triangles and the center seems to converge on a zig-zag curve towards a point not contained in the search table. The center found on the second iteration has the same search value as X_{58689}.

2.4.8 Feuerbach point X_{11}

Finally, we come to the Feuerbach point, where the Cevian construction also leads to a collapse of the triangles but with a higher numerical stability due to different operations used for construction. The center seems to converge towards a point not found in the search table before eventually also becoming unstable. The repeated pedal triangle construction results in an interesting pattern of periodically alternating between similar triangle shapes but again with numerical deviations after each iteration.

2.4.9 Search value results

As our final numerical results, we list the search value found for each center and construction type in Table 1. We used 40 iterations of repeated center construction paired with a precision of 80 digits. For better readability, we truncated values in Table 1 after 20 digits right of the decimal point. Only X_3 and X_6 lead to already known triangle centers in KIMBERLING's seach table using repeated construction from pedal triangles and are X_2 and X_{1285}, respectively.

3 Analytical framework and first results

3.1 Proper choice of coordinates

When dealing with results from Euclidean geometry, computations are preferably done in Cartesian coordinates. Therefore, we impose the frame of reference such that the vertices of the triangle $\Delta = ABC$ are given by

$$A = (0,0), \;\; B = (c,0), \;\; C = (u,v), \tag{1}$$

where u and v are subject to

$$u^2+v^2 = b^2, \;\; (u-c)^2+v^2 = a^2 \iff \\ u = \frac{1}{2c}(-a^2+b^2+c^2), \;\; v = \frac{2F}{c} \tag{2}$$

and $a = \overline{BC}$, $b = \overline{CA}$, $c = \overline{AB}$ are the side lengths of the base triangle Δ and F equals Δ's area.
This setting allows an immediate switch to (exact or homogeneous) trilinear coordinates. The y-coordinate y_P of each point (center) is the third trilinear coordinate of this particular point P, since it is the oriented distance of P to the line $[A,B]$ (the x-axis). In any case, y_P will be a function in a, b, c and, cyclically replacing them according to $a \to b$, $b \to c$, $c \to a$, turns y_P into the first trilinear coordinate function of P, *i.e.*, it becomes the trilinear distance to $[B,C]$, and so, we obtain the generating center function. This allows for a comparison with the Encyclopedia of Triangle Centers [7]. For example, the coordinates of Δ's incenter X_1 in the present coordinate system are

$$X_1 = \left(\frac{1}{2}(-a+b+c), \frac{2F}{a+b+c}\right). \tag{3}$$

	Cevian triangle	Pedal triangle
X_1	1.95770029904487735665	0.80433539504925636000
X_2	2.62936879248871824114	1.76867523171775377550
X_3	-3891699654776.25808763607293483169	2.62936879248116398887
X_4	-1.02844023546083472296	-1.02844023546083472296 4
X_5	0.76566640603164320837	1.32186957169792197941
X_6	1.09217049764661208244	0.10296691685647652550
X_7	0.80433539504925636000	0.15823641292070149571
X_8	2.53702599581424750311	1.56932209282972051791
X_9	3.12652311458376376898	2.15889133044926341090
X_{11}	2.57245781384282079537	2.17029063766605551907

	Intouch triangle of medial triangle
X_{10}	3.19337592231807969123

Table 1: *Search values per center and construction type. X_{10} uses its own special construction method. X_3 changes value after each iteration and does not seem to converge. For X_4 Cevian and pedal construction result in the same triangles. X_8, X_9, and X_{11} terminate after only a handful of iterations. The search values for X_3 and X_6 using pedal triangles are contained in* KIMBERLING's *search table and are X_2 and X_{1285}, respectively.*

Its second coordinate equals $\frac{2F}{a+b+c}$ and a cyclic shift of a, b, c does not alter it. Further, we can cut out all factors which are cyclically symmetric in a, b, c (here, they are F and $a+b+c$) and we obtain the trilinear center function of X_1 which equals 1 (cf. [7, 8]). For centers with a more intricate trilinear representation, we evaluate at the triangle with $a=6$, $b=9$, $c=13$ and compare with the respective search table on [7].

When we aim at a repeated construction of triangle centers, we have to determine a new reference triangle in each step. There are two simple but in some sense natural choices:
1. the pedal triangle $\Delta_p(X)$ of a point X whose vertices are the orthogonal projections of X onto the sides of a triangle Δ and
2. the Cevian triangle $\Delta_C(X)$ of a point X whose vertices are the projections of X from the vertices of a triangle to the opposite sides.

They will serve as the reference triangles in most of the cases we shall treat here. We shall not mix the triangles of reference from step to step, since this may cause a chaotic behaviour and no convergence will be observed.

The construction of a pedal triangle will fail for all centers X_i of Δ on the circumcircle, since these pedals lie on their respective Simson line. The Cevian triangle and the pedal triangle coincide if the chosen center equals the orthocenter X_4.

We are not restricted to the pedal triangle or the Cevian triangle. In some cases, we may choose another central triangle that may be related closer to the center that is repeatedly constructed.

3.2 Algebraic results

3.2.1 Centroid

It is not worth mentioning that the centroid X_2 is stable if we repeat the construction of the centroid always using the Cevian triangle. The Cevian triangle is the medial triangle of its predecessor in each step and all medial and medial of medial triangles are perspective to each other and the centroid X_2 serves as the perspector, while the line at infinity takes the role of the perspectrix.

In Fig. 4, the centroid X_2^{i+1} is constructed as the centroid of the pedal triangle of its predecessor. Although the polygon $X_2X_2^1X_2^2\ldots$ shows a spiraloid behaviour there is no simple generation that can easily be detected. Simulations show that the sequence of centroids converges and the search value equals $1.768675231717\ldots$, but there is no known center corresponding to that.

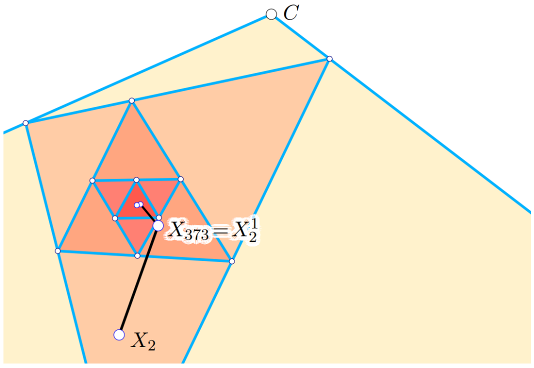

Figure 4: *The limit of $X_2^{i+1}(\Delta_p(X_2^i))$ is not yet known and the growth rules of the polygon $X_2X_2^1X_2^2\ldots$ cannot easily be read off from the figure.*

3.2.2 Incenter

The incenter of Δ is a rather nasty chum. Although it is given by $1:1:1$ in terms of homogeneous trilinear coordinates (cf. [7, 8]), for X_1 has equal (oriented) distances to Δ's sides, its Cartesian representation (3) involves square roots (since the triangles area F does). Repeating the construction of the incenter using the intouch triangle $\Delta_i=\Delta_p(X_1)$ (triangle of contact points of the incircle with the side lines of Δ) doubles the problems. Again angles have to be halved, or equivalently, unit vectors between points whose coordinates already involve square roots have to determined. The "next" incenter is that of Δ_i and is labelled X_{177} (and called the 1st *Mid-Arc Point*) in KIMBERLING's encyclopedia with the trilinear center function

$$\sqrt{bc}\sqrt{a-b+c}\sqrt{a+b-c}(\sqrt{b}\sqrt{a-b+c}+\sqrt{c}\sqrt{a+b-c})$$

(compare the equivalent trigonometric expression in [7, 8]).

As a matter of fact, X_1 always lies in the interior of Δ. Moreover it also lies in the interior of its pedal triangle $\Delta_p(X_1)=\Delta_i$, the intouch triangle (contact points of the incircle and the side lines of Δ). It also lies in the interior of its Cevian triangle $\Delta_C(X_1)$ which we shall investigate later. If we repeat the incenter construction with either Δ_i or $\Delta_C(X_1)$, we find a triangle center in the interior of the next intouch or Cevian triangle. It is clear that all these central triangles are getting smaller in each step, lie always in the interior of the preceding triangles, and it is near to assume that both Δ_i and $\Delta_C(X_1)$, and X_1 converge to a point after infinitely many construction steps. Unfortunately, the algebraic complexity even of $X_1(\Delta_i)=X_{177}$ and also of $X_1(\Delta_i(X_{177}))$ make clear that an algebraic approach towards X_1^∞ is hopeless.

Nonetheless, we can show that the intouch triangle reaches a special shape in the limit:

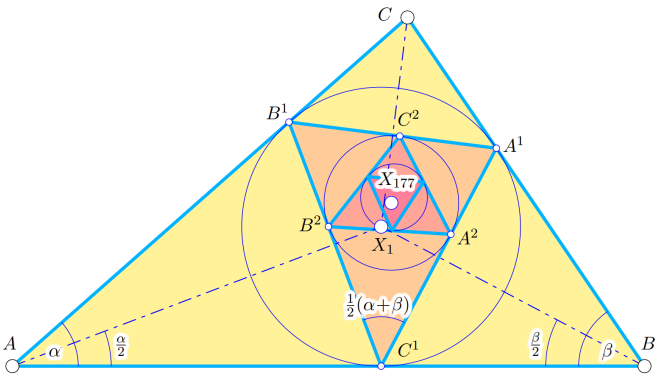

Figure 5: *The repeated construction of the intouch triangle regularizes the triangle. A limit of the incenter that is obtained as the last intouch triangle can only be found numerically.*

Theorem 1 *The repeated intouch triangle construction yields an equilateral triangle after infinitely many steps.*

Proof. We read Fig. 5 and find that $\overline{AC^1} = \overline{AB^1}$, and thus, C^1AB^1 is isosceles. Hence, $\sphericalangle AC^1B^1 = \sphericalangle AB^1C^1 = \frac{1}{2}(\pi-\alpha)$. Further, $\sphericalangle BC^1A^1 = \frac{1}{2}(\pi-\beta)$, and thus, $\gamma' := \sphericalangle A^1C^1B^1 = \frac{1}{2}(\alpha+\beta)$ and the same holds true for the other interior angles of Δ_i (with cyclic replacements of all involved objects and values). So, the interior angles of Δ and Δ_i are related by the linear mapping

$$\begin{pmatrix} \alpha' \\ \beta' \\ \gamma' \end{pmatrix} = \frac{1}{2} \begin{pmatrix} 0 & 1 & 1 \\ 1 & 0 & 1 \\ 1 & 1 & 0 \end{pmatrix} \begin{pmatrix} \alpha \\ \beta \\ \gamma \end{pmatrix}.$$

The symmetric coordinate matrix of this linear mapping can be diagonalized by $\mathbf{T}^{-1}\mathbf{L}\mathbf{T} = \mathbf{D}$, where $\mathbf{D} = \mathrm{diag}(1, -\frac{1}{2}, -\frac{1}{2})$ and the transformation matrix $\mathbf{T}$ equals

$$\begin{pmatrix} \frac{1}{3} & -\frac{1}{3} & -1 \\ \frac{1}{3} & -\frac{1}{3} & 0 \\ \frac{1}{3} & \frac{2}{3} & 1 \end{pmatrix}.$$

We can apply the linear mapping infinitely many times: $\mathbf{L}^\infty = (\mathbf{T}\mathbf{D}\mathbf{T}^{-1})^\infty = \mathbf{T}\mathbf{D}^\infty\mathbf{T}^{-1} = \mathbf{T}\mathrm{diag}(1,0,0)\mathbf{T}^{-1} = \frac{1}{3}\mathbf{U}$ where $\mathbf{U}$ is the 3×3 matrix all of whose entries are equal to 1. This means $\alpha^{(\infty)} = \frac{1}{3}(\alpha+\beta+\gamma) = \frac{\pi}{3}$ (and cyclic) which proves the theorem. □

3.2.3 Circumcenter

Some facts from the elementary geometry of the triangle along with the numerical simulation indicate the following:

Theorem 2 *The circumcenter X_3 of Δ converges towards the centroid X_2 of the base triangle Δ, provided that the pedal triangle of X_3 serves as the reference triangle in each construction step.*

Proof. The pedal triangle of X_3 equals the medial triangle Δ_m of Δ. The circumcenter of Δ_m is the nine-point center X_5 of Δ and both lie on the Euler line. Hence, the circumcenter of the pedal triangle of X_5 in Δ_m is the point X_{140} which is just called the *midpoint of X_3 and X_5* in C. KIMBERLING's Encyclopedia [7].

Consequently, X_{140} is also located on the Euler line and all further circumcenters of the respective pedal triangles gather there. Moreover, the circumcenters jump forth and back always halving the previous segment (see Fig. 6).

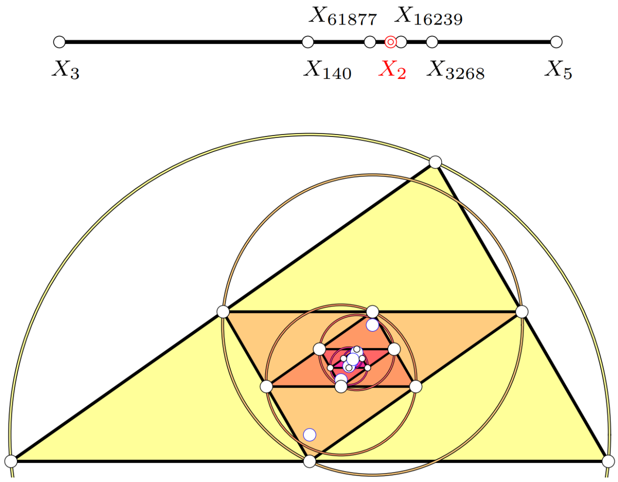

Figure 6: *The centroid is the circumcenter limit (above). Some on the initial pedal (medial) triangles with their circumcircles occuring in the limit procedure (below) share the Euler line (indicated by blue circles).*

We obtain the following sequence

$$\begin{aligned} X_3^0 &= X_3, \\ X_3^1 &= X_5, \\ X_3^2 &= \tfrac{1}{2}(X_3^1 + X_3^0) = X_{140}, \\ X_3^3 &= \tfrac{1}{4}(X_3^2 + X_3^1) = X_{3268}, \\ X_3^4 &= \tfrac{1}{8}(X_3^3 + X_3^2) = X_{16239}, \\ X_3^5 &= \tfrac{1}{16}(X_3^4 + X_3^3) = X_{61877}, \\ &\vdots \end{aligned}$$

and, expressing these affine combinations as sums of X_3^1 and X_3^0, we find

$$X_3^k = \frac{1}{2^{k-2}} \left(\mathcal{J}(k-1) X_3^{k-1} + \mathcal{J}(k) X_3^{k-2} \right),$$

where $\mathcal{J}(k) = \frac{1}{3}(2^k - (-1)^k)$ is the k-th Jacobsthal number (cf. [14]), which approaches $\frac{1}{3}2^k$ for increasing k. Now, we can find the limit point X_3^∞ as

$$\begin{aligned}&\lim_{k\to\infty} X_3^k = \\ &= \tfrac{1}{3}\lim_{k\to\infty}\tfrac{1}{2^{k-1}}\left((2^{k-1}-(-1)^{k-1}X_3^1 + (2^k-(-1)^k)X_3^0\right) = \\ &= \tfrac{2}{3}X_5 + \tfrac{1}{3}X_3 = X_2\end{aligned}$$

which completes the proof. □

From the proof of Thm. 2 we can infer:

Theorem 3 *The triangle centers X_5 (nine-point center), X_{140}, X_{3268}, X_{16239}, X_{61877}, … in this sequence converge towards the centroid X_2 of the base triangle Δ, provided that the pedal triangle and the circumcenter construction are combined in each step.*

The numerical simulation described in Sec. 2 indicates the following:

Theorem 4 *The Symmedian point X_6 converges towards the 1st Lemoine dilation center X_{1285}, provided the pedal triangle serves as the reference triangle in each step.*

Proof. In order to verify the result, we compute some instances of the Symmedian point and show that it traverses a zig-zag polygon which consists of infinitely many similar copies that terminate in X_{1285}. The first Symmedian point X_6 is that of Δ with coordinates

$$X_6 = \frac{1}{2\tau}\left(c(-a^2+3b^2+c^2), 4cF\right),$$

where $\tau := a^2+b^2+c^2$ and its pedal triangle has the vertices (in that particular order, *i.e.*, the first vertex on $[B,C]$)

$$\begin{gathered}\tfrac{1}{4c\tau}\left(c^4+8b^2c^2-b^4-(a^2-b^2)^2, 4F(a^2-b^2+3c^2)\right),\\ \tfrac{1}{4c\tau}\left((a^2-b^2-c^2)(a^2-b^2-3c^2), 4F(-a^2+b^2+3c^2)\right),\\ \tfrac{1}{2\tau}\left(c(a^2-3b^2-c^2), 0\right).\end{gathered}$$

The next Symmedian points are

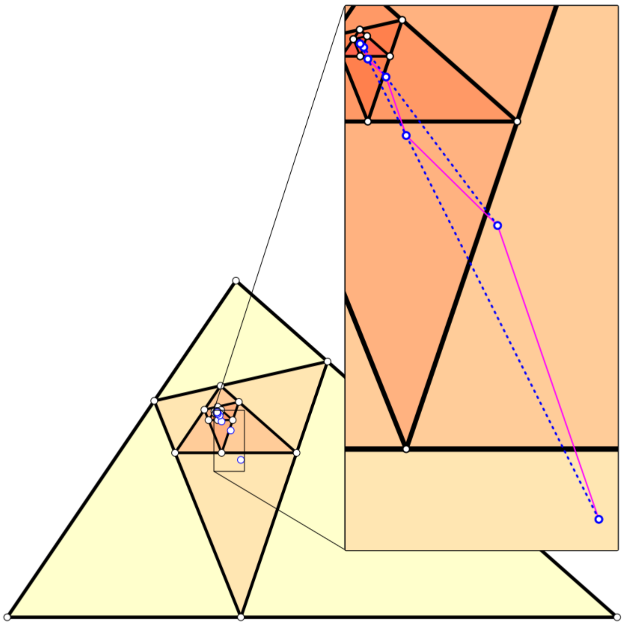

Figure 7: *The zig-zag path of the Symmedian points dithers to X_{1285}. The dotted lines joining the "even" and "odd" points intersect in the similarity center X_{1285}.*

Now, we are able to verify that the polygons $P_{012} = X_6X_6^1X_6^2$ and $P_{234} = X_6^2X_6^3X_6^4$ are similar. The scaling factor of the similarity $P_{012} \to P_{234}$ equals

$$f = \frac{12F^2}{\tau^2} = \frac{3}{4}\left(1 - \frac{2}{\tau^2}(a^4+b^4+c^4)\right) < 1.$$

The involved pedal triangles are also similar, and thus, we can be sure that the construction of any further part of the X_6^i polygon consists of pieces similar to the initial part. Instead of adding a geometric sequence of vectors, we note that the points $X_6, X_6^2, X_6^4, \ldots$ and the points $X_6^1, X_6^3, X_6^5, \ldots$ are collinear. Therefore, we intersect the lines passing through the "odd" and "even" points in order to obtain the limit

$$X_6^1 = \frac{1}{4c\tau^2}\begin{pmatrix} a^6 - a^4(3b^2+4c^2) + a^2(b^2+c^2)(3b^2+c^2) - b^6 + 8b^4c^2 + 7b^2c^4 + 2c^6 \\ -4(a^4 - a^2(2b^2+c^2) + b^4 - b^2c^2 - 4c^4)F \end{pmatrix},$$

$$X_6^2 = \frac{1}{8c\tau^3}\begin{pmatrix} a^8 - a^6(2b^2-c^2) - a^4(19b^2+17c^2)c^2 + \ldots \\ -4F\left(a^6 - a^4(b^2-4c^2) - a^2(b^2+8c^2)b^2 + \ldots\right) \end{pmatrix},$$

$$X_6^3 = \frac{1}{16c\tau^4}\begin{pmatrix} -a^{10} + a^8(13b^2+16c^2) - 2a^6(17b^4+32b^2c^2+25c^4) + \ldots \\ 4F\left(a^8 - (12b^2+13c^2) + a^4(22b^4+13b^2c^2+13c^4) + \ldots\right) \end{pmatrix},$$

$$X_6^4 = \frac{1}{32c\tau^5}\begin{pmatrix} a^{12} + 3a^{10}(4b^2+c^2) - a^8(27b^4+17b^2c^2+10c^4) + \ldots \\ -4F\left(a^{10} + a^8(13b^2+6c^2) - 2a^6(7b^4-24b^2c^2-21c^4) + \ldots\right) \end{pmatrix}.$$

point

$$L=[X_6,X_6^2]\cap[X_6^1,X_6^3]=$$
$$=\frac{1}{2c}\left(\begin{array}{c}\star\\ \dfrac{-4F(a^2-b^2-3c^2)(a^2-b^2+3c^2)}{7a^4+2a^2b^2+2a^2c^2+7b^4+2b^2c^2+7c^4}\end{array}\right).$$

Cyclically shifting a, b, c in the second coordinate function and cutting out cyclic symmetric factors (F and the quartic polnomial in the denominator) yields the generating trilinear center function

$$bc(3a^2-b^2+c^2)(3a^2+b^2-c^2)$$

and the search value 0.1029669168564765255 together with the trilinear representation given at [7] identifies this point as X_{1285}. □

References

[1] AGAOKA, Y., Degree of a Triangle Center and a Generalization of the Euler Line. *Beitr. Algebra Geom.* **51**(1) (2010), 63–89.

[2] CASEY, J., *A Sequel to the First Six Books of the Elements of Euclid*. Hodges, Figgis & co., Dublin, 1886.

[3] CHANG, G.Z., DAVIS, P.J., Iterative processes in elementary geometry. *Am. Math. Mon.* **90**(7) (1983), 421–431, https://doi.org/10.1080/00029890.1983.11971250

[4] DIXMIER, J., KAHANE, J.-P., NICOLAS, J.-L., Un exemple de non-dérivabilit'e en géométrie du triangle. *Enseign. Math.* (2) **53**(3–4) (2007), 369–428.

[5] HALBEISEN, L., HUNGERBÜHLER, N., The exponential pencil of conics. *Beitr. Algebra Geom.* **59** (2018), 549–571, https://doi.org/10.1007/s13366-017-0375-1

[6] ISMAILESCU, D., JACOBS, J., On sequences of nested triangles. *Period. Math. Hung.* **53** (2006) (1–2), 169–184, https://doi.org/10.1007/s10998-006-0030-3

[7] KIMBERLING, C., *Encyclopedia of Triangle Centers. Available at:* https://faculty.evansville.edu/ck6/encyclopedia

[8] KIMBERLING, C., Triangle Centers and Central Triangles. (*Congressus Numerantium Vol. 129*) Utilitas Mathematica Publishing, Winnipeg, 1998.

[9] KINGSTON, J.G., SYNGE, J.L., The sequence of pedal triangles. *Am. Math. Mon.* **95**(7) (1988), 609–620, https://doi.org/10.1080/00029890.1988.11972056

[10] Lax, P.D., The ergodic character of sequences of pedal triangles. *Am. Math. Mon.* **97**(5) (1990), 377–381, https://doi.org/10.1080/00029890.1990.11995610

[11] MICROSOFT, *Floating-point numeric types - C# reference.* Available at: https://learn.microsoft.com/en-us/dotnet/csharp/language-reference/builtin-types/floating-point-numeric-types

[12] ODEHNAL, B., Poristic loci of triangle centers. *J. Geom. Graph.* **15**(1) (2011), 45–67.

[13] ODEHNAL, B., Two Convergent Triangle Tunnels. *KoG* **22** (2018), 3–11, https://doi.org/10.31896/k.22.1

[14] SLOANE, N.J.A.. *The On-Line Encyclopedia of Integer Sequences (OEIS).* Available at: https://oeis.org

[15] WHITE, A., *BigDecimal: An arbitrary-precision decimal (base 10) floating-point number class*. Available at: https://github.com/AdamWhiteHat/BigDecimal

Christian Clemenz
e-mail: christian.clemenz@uni-ak.ac.at
University of Applied Arts Vienna
Oskar-Kokoschka-Platz 2, A-1010 Vienna, Austria

Boris Odehnal
orcid.org/0000-0002-7265-5132
e-mail: boris.odehnal@uni-ak.ac.at
University of Applied Arts Vienna
Oskar-Kokoschka-Platz 2, A-1010 Vienna, Austria